
SYNTHESIS AND PROPERTIES OF INORGANIC COMPOUNDS

Synthesis of $\text{Ba}_4\text{R}_3\text{F}_{17}$ (R stands for Rare-Earth Elements) Powders and Transparent Compacts on Their Base

S. V. Kuznetsov, P. P. Fedorov, V. V. Voronov, K. S. Samarina,
R. P. Ermakov, and V. V. Osiko

*Research Center for Laser Materials and Technologies,
Prokhorov Institute of General Physics, Russian Academy of Sciences,
ul. Vavilova 38, Moscow, 119991 Russia*

e-mail: ksv@lst.gpi.ru

Received June 26, 2009

Abstract—Single-phase samples of $\text{Ba}_4\text{R}_3\text{F}_{17} \cdot n\text{H}_2\text{O}$ (R = La, Ce, Pr, Nd, Eu, Gd, Y, Er, or Yb; $n = 2.5–3.2$) were prepared by coprecipitation from nitrate solutions using hydrofluoric acid. The phases crystallize in a fluorite-type face-centered cubic lattice. The dried precipitates are transparent. Scanning electron and atomic-force microscopy and X-ray diffraction line broadening show a hierarchic structure in the samples: primary nanoparticles join into agglomerates with characteristic sizes of about 150–200 nm, these agglomerates being self-packed into parallel layers with a thickness on the order of 500 nm.

DOI: 10.1134/S0036023610040029

Barium fluoride-based solid solutions with rare-earth fluorides $\text{Ba}_{1-x}\text{R}_x\text{F}_{2+x}$ (R = TR) have long been known and widely used in various sciences and technologies. These materials are produced mostly as single crystals [1, 2] or ceramics [3]. However, there are various obstacles to the synthesis of heavily doped single crystals and ceramics based on barium fluoride. Single crystal growth is complicated by growth defects (cellular substructure and striation) [4]. Ceramic synthesis requires the use of concentration-homogeneous powders, as the quality of the precursor powders directly influences the optical parameters of the resulting ceramics.

BaF_2-RF_3 systems were addressed repeatedly. Sobolev and Tkachenko [5] plotted phase diagrams over the range from melting temperatures to 800°C for R = Sm–Lu and to 900°C for R = La–Nd. Extensive fields of $\text{Ba}_{1-x}\text{R}_x\text{F}_{2+x}$ solid solution with a fluorite structure (space group $Fm\bar{3}m$) are formed in all systems; their maximal extent is $x = 0.50 \pm 0.02$ for R = La–Nd and shrinks as the rare earth ionic radius decreases. Fluorite-like phases of variable composition $\text{Ba}_{4\mp x}\text{R}_{3\pm x}\text{F}_{17\pm x}$ having a fluorite-derived structure (hexagonal space group $R\bar{3}$), which exist in the concentration range of 40–45 mol % RF_3 , were revealed in the systems with R = Sm–Lu. These phases melt incongruently where R = Tb–Lu and decompose in a solid state where R = Sm–Gd. A polymorphic transition from a hexagonal to tetragonal phase was observed, as temperature increased, for R =

Sm–Tb. Maksimov et al. [6] considered in detail the crystal structure of $\text{Ba}_{4\mp x}\text{R}_{3\pm x}\text{F}_{17\pm x}$ phases with R = Y and Yb, verifying that their structure is hexagonal with an ideal formula of $\text{Ba}_4\text{R}_3\text{F}_{17}$. This hexagonal structure was shown to be a distortion of the barium fluoride cubic lattice. By means of long anneals at temperatures in the range 1000–400°C, Kieser and Greis [7] synthesized a series of $\text{Ba}_4\text{R}_3\text{F}_{17}$ compounds, including those for R = Ce–Nd, which were not mentioned by Sobolev and Tkachenko [5]. For R = La such a phase has not been prepared. Prituzhalov et al. [8] studied phase equilibria in the $\text{BaF}_2-\text{NdF}_3$ system at 600°C. Compared to Sobolev and Tkachenko's data [5], Prituzhalov et al. noticed a dramatic shrinkage of the existence field of $\text{Ba}_{1-x}\text{Nd}_x\text{F}_{2+x}$ solid solution on account of the appearance of a $\text{Ba}_{4\mp x}\text{R}_{3\pm x}\text{F}_{17\pm x}$ ordered phase at this temperature.

Methods for the synthesis of nanofluorides are reviewed in [9]. This review mentions a gap concerning the synthesis of heavily doped barium fluoride-based solid solutions; multiphase samples are frequently obtained. Data on the synthesis of powder calcium fluoride and strontium fluoride solid solutions doped with rare earths and barium fluoride solid solutions lightly doped with rare earths (<1 mol %) by means of coprecipitation from aqueous solutions are compiled in [10]. According to these data, the method is unsuitable for synthesizing heavily doped $\text{Ba}_{1-x}\text{R}_x\text{F}_{2+x}$ solid solutions. The lack of data on the synthesis of heavily doped and homogeneous barium fluoride

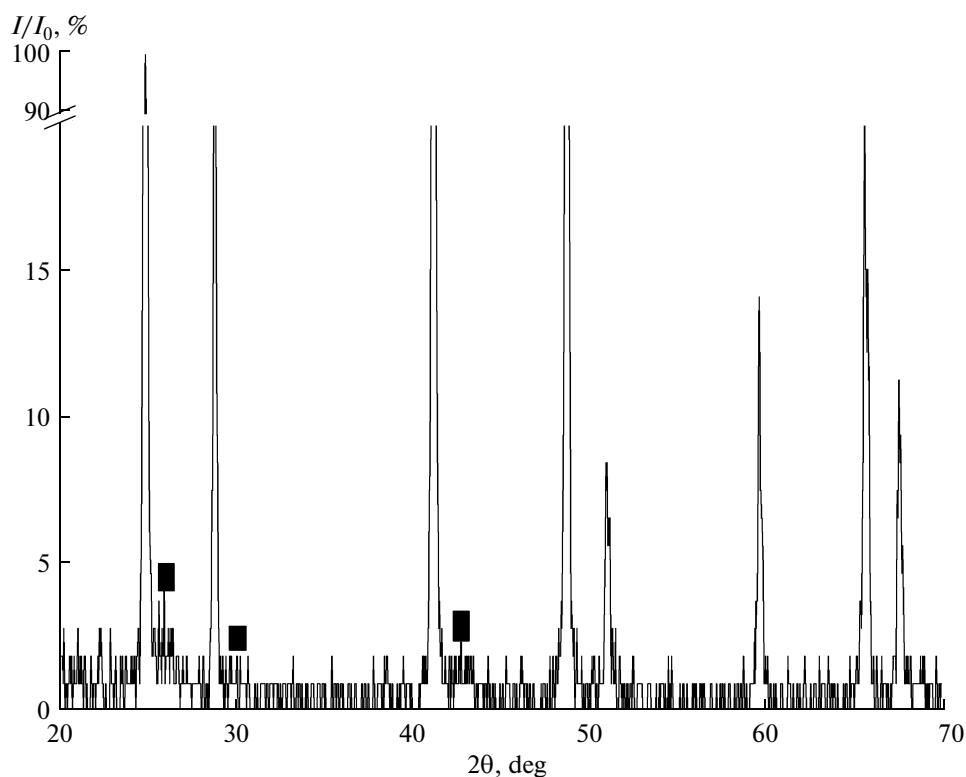


Fig. 1. X-ray diffraction pattern for a two-phase powder precipitated from a nitrate solution with the ratio Ba : Er = 99 : 1. Strong lines refer to virtually pure barium fluoride. Squares refer to a $\text{Ba}_{4+\pm x}\text{R}_{3-\pm x}\text{F}_{17-\pm x}$ phase.

powders containing rare earths and high demand for them make this study topical.

In this context, our work develops a process for preparing single-phase rare earth-doped barium fluoride powders for use in optical ceramic technology.

Table 1. Parameters of samples having the as-batch composition Ba₄R₃F₁₇

R	$a, \text{\AA}$	D, nm	$e \times 10^3$
La	6.0571	102	5.4
Ce	6.0291	>200	4.3
Pr	6.0236	>300	4.4
Nd	5.9901	>200	2.4
Eu	5.9241	>300	2.5
Gd	5.9511	>300	2.4
Y	5.8921	46	6.1
Er	5.8531	46	8.8
Yb	5.8481	19	8.7

EXPERIMENTAL

The starting materials used were as follows: Ba(NO₃)₂ (high purity grade 10–2) La(NO₃)₃ · 5H₂O (chemically pure grade), Ce(NO₃)₃ · 6H₂O (chemically pure grade), Pr(NO₃)₃ · 6H₂O (99.99 grade), Nd₂O₃ prepared by calcining Nd(OH)₃ (chemically pure grade) at 810°C for 2 h, Gd(NO₃)₃ · 6H₂O (99.99 grade), Y(NO₃)₃ · 6H₂O (99.99 grade), Y₂O₃ (chemically pure grade), Er₂O₃ (chemically pure grade), Yb(NO₃)₃ · 6H₂O (99.99 grade), Yb₂O₃ (chemically pure grade), 40% HF (chemically pure grade), concentrated aqueous HNO₃ (pure for analysis grade),

Table 2. Calculated compositions of Ba₄R₃F₁₇ · nH₂O crystal hydrates

Composition	Weight percent of H ₂ O	Volume percent of H ₂ O
Ba ₄ Y ₃ F ₁₇ · 2.5H ₂ O	4.0	18.0
Ba ₄ Yb ₃ F ₁₇ · 3.2H ₂ O	4.0	21.3

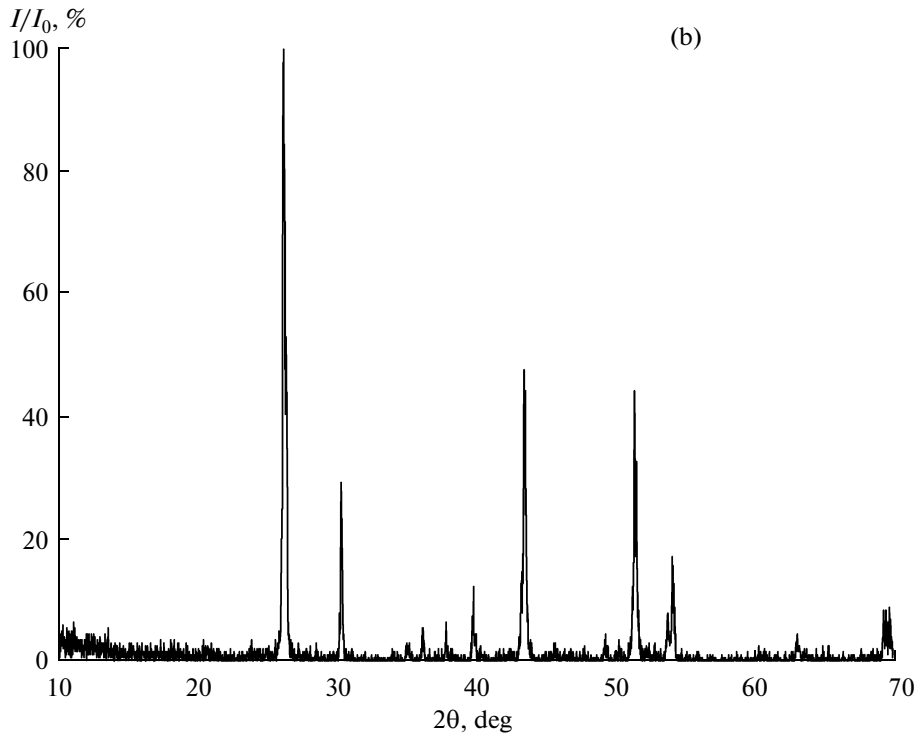
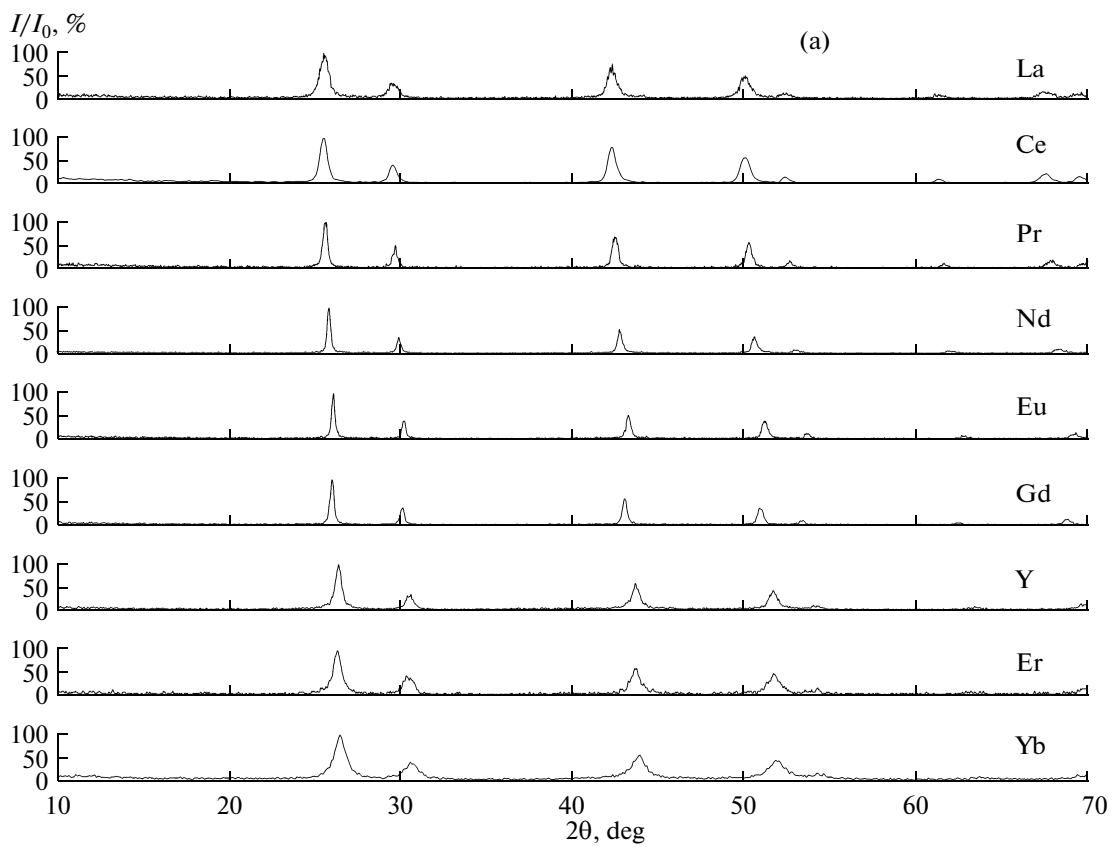


Fig. 2. X-ray powder diffraction patterns for (a) powders of as-batch composition Ba₄R₃F₁₇, where R = La, Ce, Pr, Nd, Eu, Gd, Y, Er, or Yb, prepared by precipitation from nitrate solutions; and (b) an ordered Ba₄Y₃F₁₇ phase prepared by solid-phase synthesis.

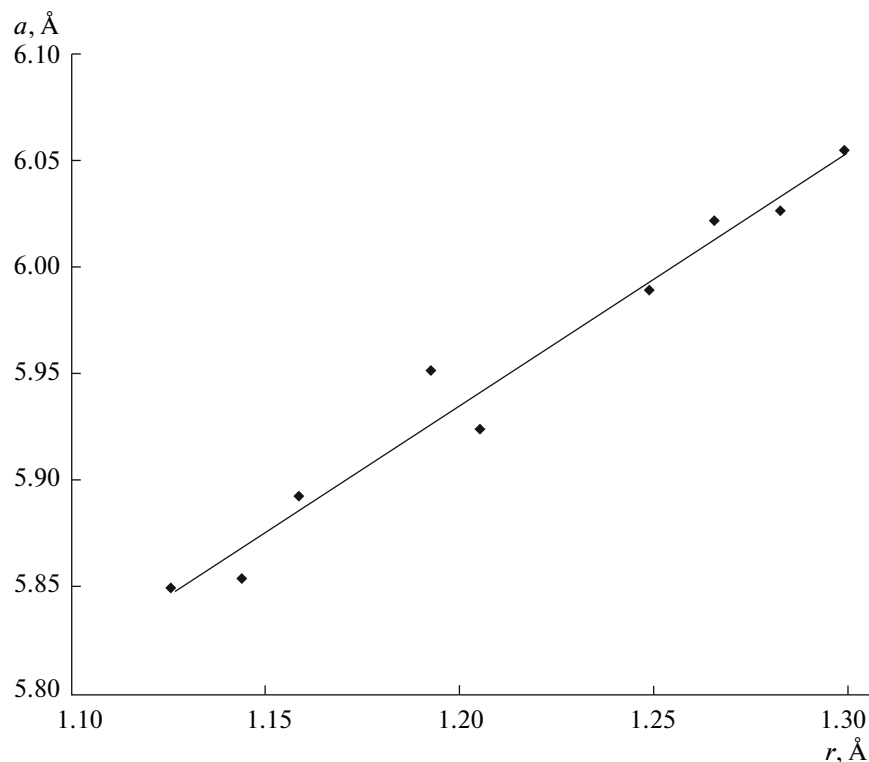


Fig. 3. Unit cell parameter vs. doping rare-earth radius [12] for precipitated Ba₄R₃F₁₇ phases. Line: $a = 1.2061r + 4.488$; correlation coefficient: $R = 0.986$.

30% NH₄OH solution (pure for analysis grade), and distilled water.

For syntheses, barium nitrate and rare-earth nitrate solutions were prepared from relevant nitrates or oxides (by dissolving the oxides in nitric acid) with set Ba : R ratios. The barium nitrate concentration was 0.1 mol/L. The thus prepared solutions were combined and dropped to aqueous hydrofluoric acid under stirring. The resulting suspension was allowed to settle, decanted, and neutralized by aqueous ammonia to pH ≈ 5, and then washed with distilled water several times. The precipitate was allowed to settle, collected on a filter, and then dried below 100°C.

Powders synthesized as set forth were studied by X-ray diffraction on DRON-4M diffractometer using CuK_α radiation with pyrolytic graphite monochromator (to perform phase analysis) and URD-63 diffractometer (to determine crystallite sizes as coherent scattering domain sizes and microstrains), atomic force microscopy on a Solver P47 scanning probe microscope in the intermittent contact mode in air, scanning electron microscopy on a Supra 50 VP microscope, and thermogravimetry on a Q 1500D thermal analyzer. Unit cell parameters were calculated using Powder 2.0 software. The calculation error did not exceed 0.002 Å. The coherent scattering domain

sizes and microstrains were determined as described in [11]. A reference was a powder obtained by triturating a BaF₂ single crystal with ethanol (with an agate mortar and pestle) for 30 min. X-ray diffraction peak parameters (position, area, and width) were determined using Microcal Origin software.

RESULTS AND DISCUSSION

Figure 1 illustrates the problem of synthesis of heavily doped barium fluoride-base solid solutions of rare-earths. X-ray diffraction patterns for samples prepared by coprecipitation of barium fluoride and rare-earth fluorides under the action of hydrofluoric acid contains, along with lines from virtually pure cubic barium fluoride, low-intensity peaks also referring to a fluorite-type lattice, but with far smaller unit cell parameters. Calculating the unit cell parameters for this second phase in the cubic approximation, we identified it as a phase having an idealized formula unit of Ba₄Er₃F₁₇. The distinction from the results of the synthesis of solid solutions based on calcium and strontium fluorides (in those systems, single-phase samples were obtained) may arise from a greater difference between the solubilities of barium fluoride and rare-earth fluorides. The sets of reflections observed in the X-ray diffraction patterns associated with fluorite-

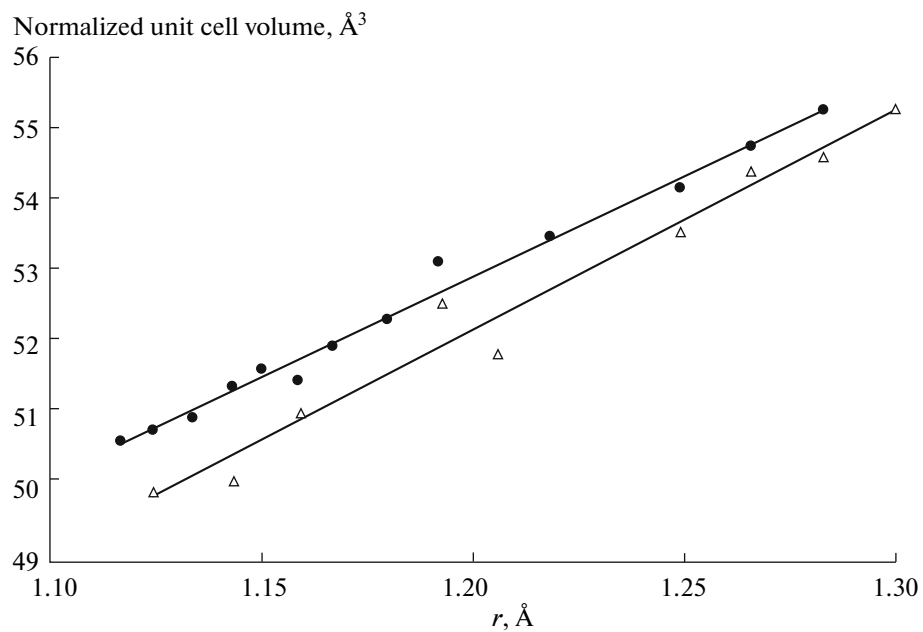


Fig. 4. Normalized unit cell volume vs. rare-earth radius for $\text{Ba}_4\text{R}_3\text{F}_{17}$ phases formulated as $(\text{Ba}, \text{R})\text{F}_{2+x}$. Circles show data borrowed from [7]; triangles show our data. The relevant regression equations are as follows: for our data, $V = 31.97r + 13.796$, $R = 0.986$; for data borrowed from [7], $V = 29.382r + 17.63$, $R = 0.995$.

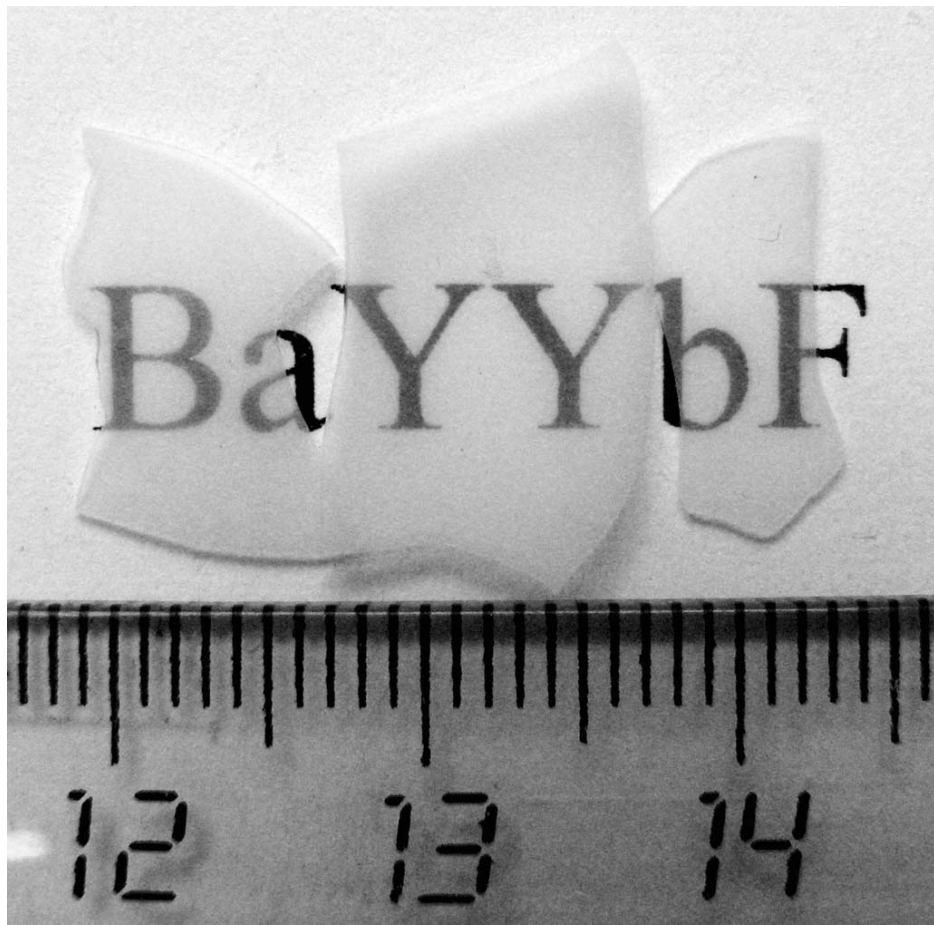


Fig. 5. Transparent compacts of as-batch composition $\text{Ba}_4(\text{Y}_{0.9}\text{Yb}_{0.1})_3\text{F}_{17}$. Thickness: 1 mm.

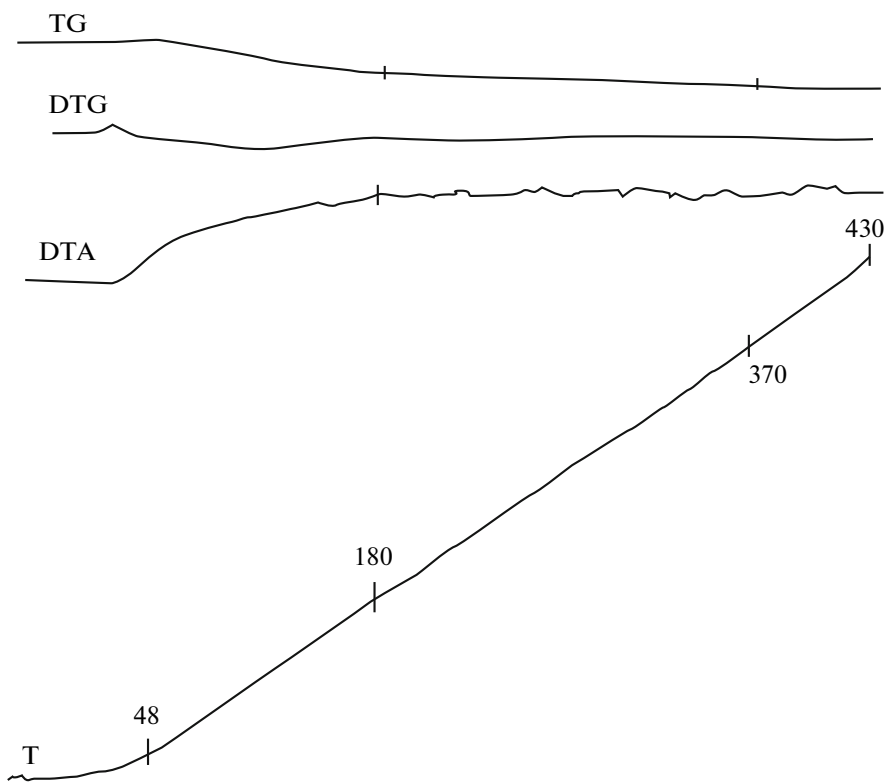


Fig. 6. Thermal curves for a sample of as-batch composition $\text{Ba}_4\text{Y}_3\text{F}_{17}$: T—temperature curve, DTA—differential temperature curve, DTG—differential weight curve, TG—weight curve. Heating rate: 10 K/min; sample size: 340 mg; Alundum crucible.

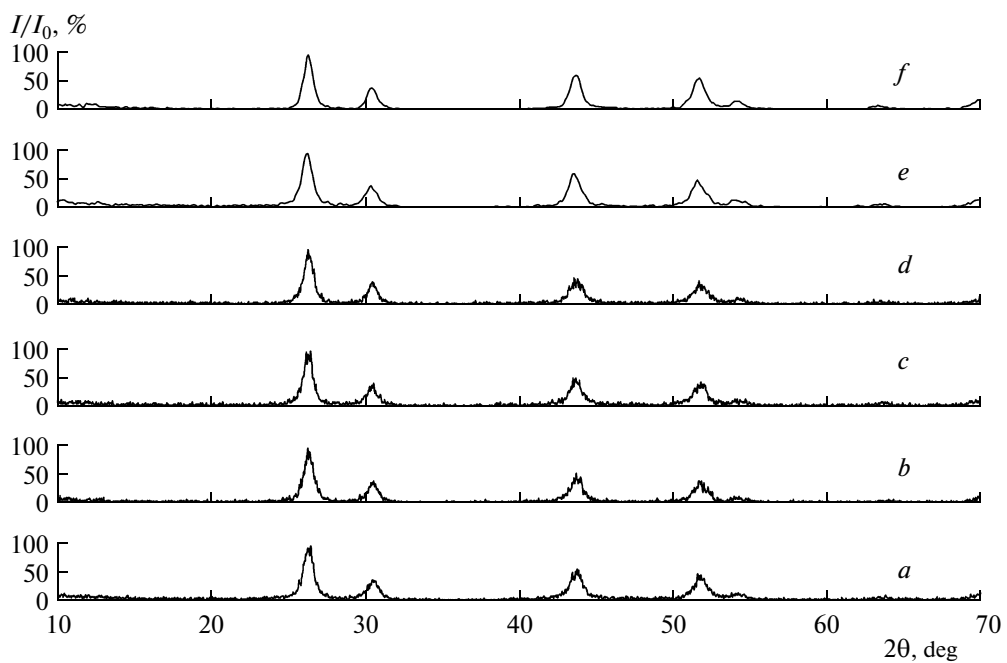


Fig. 7. X-ray diffraction patterns for samples of as-batch composition $\text{Ba}_4\text{Yb}_3\text{F}_{17}$ after heat treatment: (a) an untreated transparent compact dried at temperatures below 100°C; and (b–f) samples heated to 200, 250, 350, 430, 450°C, respectively.

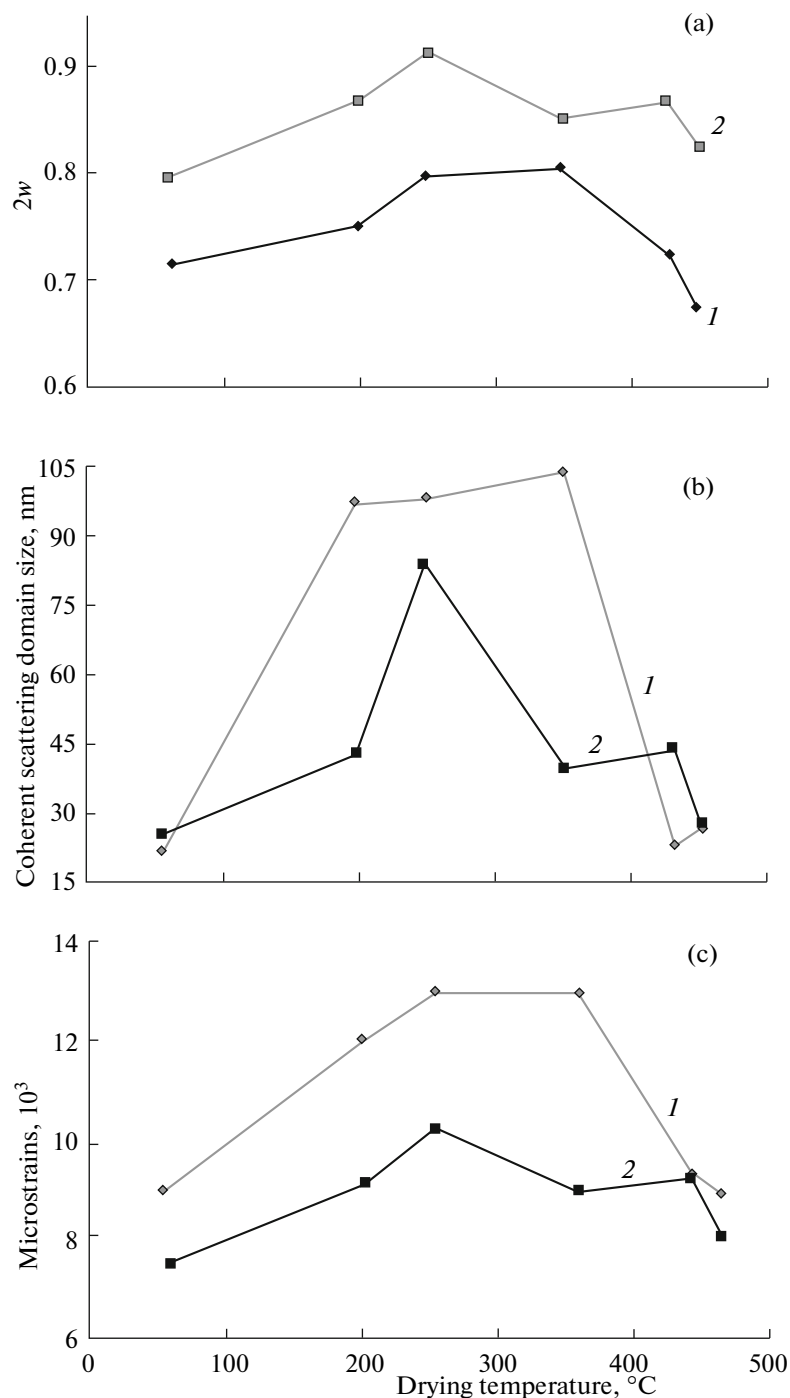


Fig. 8. X-ray diffraction parameters of samples of as-batch composition $\text{Ba}_4\text{Yb}_3\text{F}_{17}$ vs. heat treatment temperature: (a) peak full width at half-height, (b) coherent scattering domain size D , and (c) microstrains e . (1) (200) reflections and (2) (220) reflections.

like phases with small unit cell parameters allow us to suggest as follows: under the conditions of precipitation from nitrate solutions in the BaF_2 – RF_3 systems, $\text{Ba}_4\text{R}_3\text{F}_{17}$ compounds are the least soluble phases and are the first to form. Thus, it becomes possible to

obtain single-phase products of this composition upon coprecipitation.

Our experiments showed that the use of precursor solutions with the ratio $\text{Ba} : \text{R} = 4 : 3$ results in single-phase reaction products. Representative X-ray diffrac-

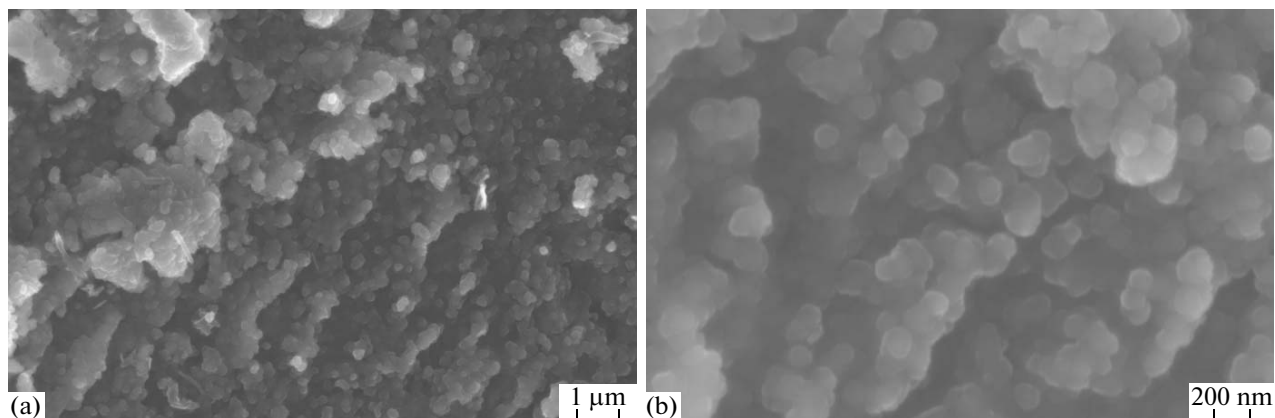


Fig. 9. SEM image of a transparent compact obtained from a Ba₄Y₃F₁₇ powder: (a) $\times 25000$ and (b) $\times 100000$.

tion patterns are shown in Fig. 2; selected parameters of synthesized samples are listed in Table 1.

All X-ray diffraction patterns recorded for the powders synthesized refer to a face-centered cubic lattice (a fluorite-type structure). No signatures of a trigonal distortion of the cubic lattice were observed nor superstructural lines characteristic of ordered Ba₄R₃F₁₇ phases. The unit cell parameter of the samples synthesized is a linear function of R³⁺ ion radius (Fig. 3). Shannon's fluoride ion radii [12] for rare earths with CN 8 were used. The unit cell parameters as determined are close to the parameters of the fluorite subcell of Ba₄R₃F₁₇ phases. Figure 4 compares our data with Kieser and Greis' data [7]; for this reason, we calculated specific volumes referring to the (Ba,R)F_{2+x} formula unit. Systematically, the cubic phases synthesized from aqueous solutions have smaller volumes than those of hexagonal phases synthesized by solid-phase reactions.

Practical applications not always require high doping levels. We carried out a set of experiments on the synthesis of so-called matrix phases doped with targeted rare-earth fluorides exemplified by Ba₄La₃F₁₇:Ce (0.5 mol %), Ba₄Gd₃F₁₇:Ce (0.5 mol %), and Ba₄(Y_{0.9}Yb_{0.1})₃F₁₇; these experiments verified the validity of our strategy of the synthesis of single-phase solid solutions. Extra reflections were not noticed in the X-ray diffraction patterns.

Noteworthy, mild drying of the precipitates (<100°C) systematically yielded transparent compacts (Fig. 5), which did not lose transparency when stored in air for several months. While being dried in air at temperatures above 100°C, compacts acquire white color but lose transparency. The attendant increase in the unit cell parameter is insignificant (0.01–0.015 Å).

The thermal stability of reaction products was determined in thermoanalytical experiments on sam-

ples of as-batch compositions Ba₄Y₃F₁₇ and Ba₄Yb₃F₁₇. Heating was carried out in air at a rate of 10 K/min (Fig. 6). The main weight change occurred before reaching 200°C and was evidently associated mainly with dehydration. Further insignificant weight change (apparently, removal of nitrates and ammonium compounds) ended at ~400°C. The weight change values were used to estimate the composition of the crystal hydrates and the bulk content of crystal water (Table 2). The water content of the samples is considerable, possibly being responsible for the transparency of the compacts.

We should mention that, although having considerable water contents, the compacts did not crack and did not lose optical transparency when immersed into liquid nitrogen. The nature of water that does not crystallize at 77 K is to be studied further.

The thermal stability of the sample of as-batch composition Ba₄Yb₃F₁₇ · 3.2H₂O was studied by X-ray diffraction. Transparent compacts were heat treated in air at various temperatures. The heating rate was 10 K/min. Once the set temperature was reached, the sample was taken from the furnace; in the experiment at 450°C, the sample was exposed for 20 min.

Peak widths at half-heights ($2w$) and integral widths (β) for (200) and (220) reflections were derived from X-ray diffraction patterns (Fig. 7), and then used to calculate coherent scattering domain sizes D and microstrains e . In choosing these reflections we were guided by the following considerations. The samples synthesized from aqueous solutions likely have a cubic structure, whereas the stable phase of this composition is hexagonal, which may be regarded as a distortion of the cubic structure. If the hexagonal distortion of the cubic lattice is the case, the initial (200) reflection is not split and the (220) reflection should be split into a pair of reflections. Figure 8, curves 1 and 2, respec-

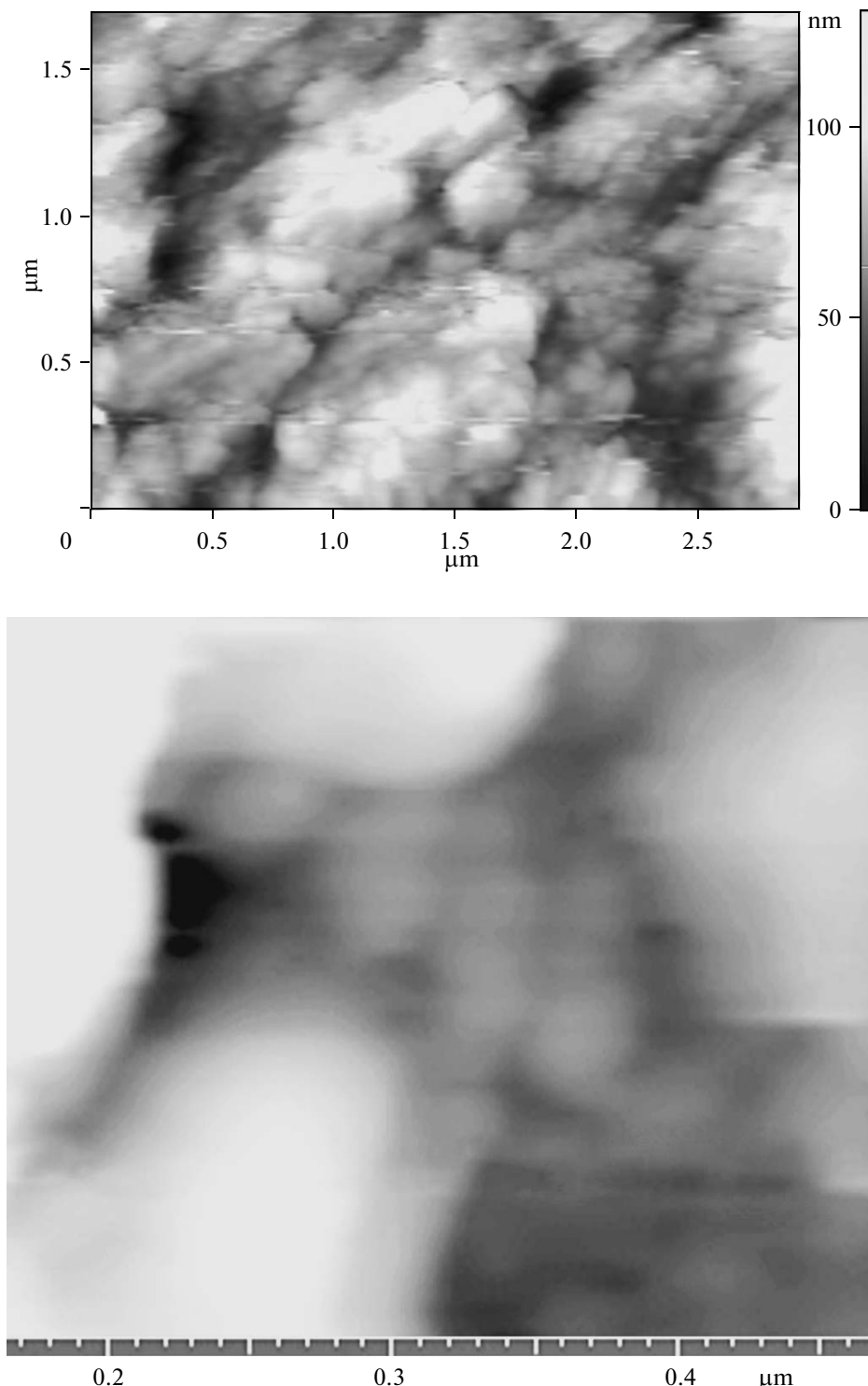


Fig. 10. AFM image of a transparent compact of a $\text{Ba}_4\text{Yb}_3\text{F}_{17}$ powder.

tively, displays $2w$, D , and e as a function of drying temperature for the (200) and (220) reflections of the fluorite lattice.

Figure 8 demonstrates the broadening of the (220) reflection relative to the (200) reflection. This broadening possibly signifies the hexagonal distortion of the

cubic lattice, which might remained unnoticed because of peak broadening caused by small particle sizes.

The samples synthesized were studied using scanning electron and atomic force microscopy. Figure 9 displays micrographs of a transparent compact of as-

batch composition Ba₄Y₃F₁₇. Particles packed in parallel columns are distinguished in Fig. 9a, and agglomerates with average sizes of ~150 nm are seen in Fig. 9b. From X-ray diffraction data, a value of 34 nm was derived for the coherent scattering domain size with microstrains of 4.86×10^{-3} .

Figure 10 shows AFM images of transparent compacts of a Ba₄Yb₃F₁₇ powder. Large agglomerates of particles are seen in Fig. 10a, and small particles constituting agglomerates are distinguished in Fig. 10b. A value of $D = 25$ nm was derived for $e = 7.4 \times 10^{-3}$ for the compacts shown in Fig. 10 proceeding from X-ray diffraction data, corresponding to the size of small particles distinguished by AFM.

The examination of the AFM and SEM images in Figs. 9 and 10 brings implies a hierarchic packing of nanoparticles in such the compacts, which results in their transparency. Under mild drying conditions nanoparticles join together to form agglomerates with characteristic sizes of about 150–200 nm, which are then self-packed into parallel layers ~500 nm thick.

Thus, we have not gained unambiguous evidence of the existence of trigonal distortion in our synthesized samples. Presumably, crystal water stabilizes a disordered structure. By our data, however, even dehydration at 450°C does not lead to trigonal distortion and structure ordering.

We should mention that a Ba₄La₃F₁₇ phase has not been synthesized hitherto. We cannot rule out, however, that this phase can exist below 400°C (the lowest annealing temperature used by Kieser and Greis [7]). Our synthesized sample may also correspond to a composition from the region of Ba_{1-x}R_xF_{2+x} disordered fluorite solid solution. At room temperature, however, the solid solution of this composition cannot be stable.

ACKNOWLEDGMENTS

The authors thank V.K. Ivanov, Candidate of Science in Chemistry, and O.V. Karban', Candidate of

Science in Physics and Mathematics, for performing scanning electron and atomic force microscopy experiments, respectively; O.K. Alimov, Candidate of Science in Physics and Mathematics, for recording transmission spectra at 77 and 300 K; and E.V. Chernova for photographing. S.V. Kuznetsov appreciates support from the Russian Science Support Foundation. This work was supported by the State Contract no. 02.513.12.3029 and the Russian Foundation for Basic Research (project no. 08-03-12080ofi).

REFERENCES

1. P. P. Fedorov and V. V. Osiko, *Bulk Crystal Growth of Electronic, Optical and Optoelectronic Materials*, Ed. by P. N. Y. Capper (Wiley, New York, 2005), p. 339.
2. B. P. Sobolev, Z. I. Zhmurova, V. V. Karelina, et al., in *Growth of Crystals* (Nauka, Moscow, 1988), Vol. 16, p. 58 [in Russian].
3. S. Kh. Batygov, L. S. Bolyasnikova, A. E. Garibin, et al., Dokl. Akad. Nauk **422** (2), 323 (2008).
4. S. V. Kuznetsov and P. P. Fedorov, Inorg. Mater. **44** (13), 1434 (2008).
5. B. P. Sobolev and N. L. Tkachenko, J. Less-Common Met. **85**, 155 (1982).
6. B. A. Maksimov, Kh. Solans, A. P. Dudka, et al., Kristallografiya **41** (1), 51 (1996) [Crystallogr. Rep. **41** (1), 50 (1996)].
7. M. Kieser and O. Greis, Z. Anorg. Allg. Chem. **469**, 164 (1980).
8. V. A. Prituzhalov, K. N. Zolotova, E. V. Khomyakova, et al., *Proceedings of the 4th All-Russia Conference "Physicochemical Processes in Condensed Media and at Interphases" (FAGRAN-2008)* (Nauchnaya kniga, Voronezh, 2008), Vol. II, p. 640 [in Russian].
9. S. V. Kuznetsov, V. V. Osiko, E. A. Tkachenko, and P. P. Fedorov, Russ. Chem. Rev. **75** (12), 1065 (2006).
10. S. V. Kuznetsov, I. V. Yarotskaya, P. P. Fedorov, et al., Zh. Neorg. Khim. **52** (3), 364 (2007) [Russ. J. Inorg. Chem. **52** (3), 315 (2007)].
11. D. Louer, T. Bataille, T. Roisnel, and J. Rodriguez-Carvajal, Powder Diffraction. **17** (4), 262 (2002).
12. R. D. Shannon, Acta Crystallogr., Sect. A **32** (5), 751 (1976).
13. P. P. Fedorov and B. P. Sobolev, Kristallografiya **37** (5), 1210 (1992).